Experimental Results for the Rotordynamic Characteristics of Leakage Flows in Centrifugal Pumps

A. Guinzburg

C. E. Brennen

A. J. Acosta

T. K. Caughey

California Institute of Technology,
Division of Engineering and Applied Science,
Pasadena, CA 91125

In recent years, increasing attention has been given to fluid-structure interaction problems in turbomachines. The present research focuses on just one such fluid-structure interaction problem, namely, the role played by fluid forces in determining the rotordynamic stability and characteristics of a centrifugal pump. The emphasis of this study is to investigate the contributions to the rotordynamic forces from the discharge-to-suction leakage flows between the front shroud of the rotating impeller and the stationary pump casing. An experiment was designed to measure the rotordynamic shroud forces due to simulated leakage flows for different parameters such as flow rate, shroud clearance, face-seal clearance and eccentricity. The data demonstrate substantial rotordynamic effects and a destabilizing tangential force for small positive whirl frequency ratios; this force decreased with increasing flow rate. The rotordynamic forces appear to be inversely proportional to the clearance and change significantly with the flow rate. Two sets of data taken at different eccentricities yielded quite similar nondimensional rotordynamic forces indicating that the experiments lie within the linear regime of eccentricity.

1 Introduction

In turbomachinery, the trend toward higher speeds and higher power densities has led to an increase in the number and variety of fluid-structure interaction problems in pumps, compressors, turbines and other machines. This occurs because the typical fluid forces scale like the square of the speed and thus become increasingly important relative to the structural strength. This becomes particularly acute in rocket engine turbopumps where demands to minimize the turbopump mass may also lead to reductions in the structural strength. Consequently designers and manufacturers are concerned with the fluid-induced rotordynamic forces on impellers in turbomachines. Knowledge of the steady and unsteady forces and the associated rotordynamic coefficients is required to effectively model the rotordynamics of high speed turbomachines.

2 Background

Rotordynamic forces imposed on a centrifugal pump by the fluid flow through it were first measured by Domm and Hergt (1970), Hergt and Krieger (1969–70), Chamieh et al. (1985) and Jery et al. (1985). In the Rotor Force Test Facility (RFTF) at Caltech (Jery et al., 1985; Adkins et al., 1988; Franz et al., 1989) known whirl motions over a full range of frequencies (subsynchronous, supersynchronous as well as reverse whirl) are superimposed on the normal motion of an impeller.

The hydrodynamic force on a rotating shroud or impeller (see Fig. 1) which is whirling can be expressed in the stationary laboratory frame in linear form as:

$$\begin{bmatrix} F_x^*(t) \\ F_y^*(t) \end{bmatrix} = \begin{bmatrix} F_{ox}^* \\ F_{oy}^* \end{bmatrix} + [A^*] \begin{bmatrix} x^*(t) \\ y^*(t) \end{bmatrix} \tag{1}$$

The first term on the right-hand side represents the radial force in the absence of whirl motion, so that F_{ox}^*, F_{oy}^* are the steady, time-averaged forces in a stationary frame which result from flow asymmetries in the volute or the inlet duct. These

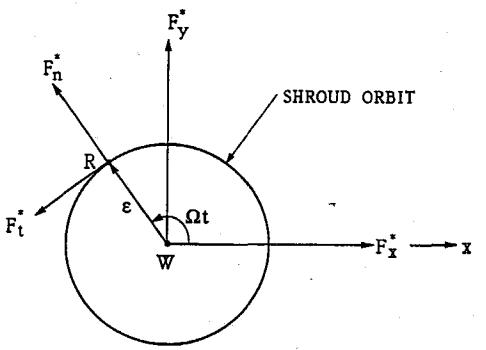

Fig. 1 Schematic of the fluid-induced radial forces acting on an impeller whirling in a circular orbit. F_x^* and F_y^* represent the instantaneous forces in the stationary laboratory frame. F_n^* and F_t^* are the forces normal and tangential to the whirl orbit where Ω is the whirl frequency.

Contributed by the Fluids Engineering Division for publication in the JOURNAL OF FLUIDS ENGINEERING. Manuscript received by the Fluids Engineering Division April 21, 1992; revised manuscript received April 22, 1993. Associate Technical Editor: S. B. Zakem.

steady radial forces are discussed in detail elsewhere (Iverson et al., 1960; Domm and Hergt, 1970; Chamieh, 1983; Chamieh et al., 1985; Adkins, 1986). The matrix $[A^*]$ is the rotordynamic matrix which operates on the instantaneous displacement $[x^*]$ of the rotor center. Note that $[A^*]$ will in general be a function not only of the mean flow conditions and pump geometry but also of the frequency of whirl, Ω. If outside the linear range, it may also be a function of the amplitude of the whirl motion, ϵ. At small, linear amplitudes $[A^*]$ should be independent of ϵ and presented as a function of the whirl frequency ratio, Ω/ω. In the case of a circular whirl orbit $x^* = \epsilon \cos \Omega t$, $y^* = \epsilon \sin \Omega t$. Then the forces normal and tangential to the imposed circular whirl orbit are related to the matrix elements as follows:

$$F_n^*(t) = \frac{1}{2}(A_{xx}^* + A_{yy}^*)\epsilon$$

$$F_t^*(t) = \frac{1}{2}(-A_{xy}^* + A_{yx}^*)\epsilon \tag{2}$$

The reader is referred to Jery et al. (1985) and Franz et al. (1989) for details. In the analysis which follow, the above equations will be expressed in nondimensional terms. If, in addition, $[A]$ is to be rotationally invariant, then

$$A_{xx} = A_{yy} = F_n$$

$$A_{xy} = -A_{yx} = F_t \tag{3}$$

The experimental investigation of Jery et al. (1985) and the fluid mechanical model of Adkins et al. (1988) for centrifugal pump impellers demonstrated that there are two sources for these fluid-induced forces. It was recognized that contributions to the rotordynamic forces could arise not only from azimuthally nonuniform pressures in the discharge flow acting on the impeller discharge area but also from similar nonuniform pressures acting on the exterior of the impeller front shroud as a result of the leakage flow passing between this shroud and the pump casing. The tentative conclusion was that the leakage flow contribution to the normal force was about 70 percent of the total and the contribution to the tangential force was about 30 percent of the total. These substantial contributions of the leakage flow to rotordynamic forces motivated this study.

There are several other indications which suggest the importance of leakage flows to the fluid-induced rotordynamic forces. It is striking that the total rotordynamic forces measured by Bolleter et al. (1987) from Sulzer Brothers, Ltd., for a conventional centrifugal pump configuration are about twice the magnitude of those measured by Jery (1986) or Adkins (1986) at Caltech. Both test programs used a radial face seal to minimize the forces which would be developed by the wear-ring seals. So the measured hydrodynamic forces are due to a combination of the impeller-volute and the impeller-shroud interaction. It now seems sensible to suggest that this difference is due to the fact that the clearance in Bolleter's leakage flow annulus is substantially smaller than that in the experiments of Jery (1986) and Adkins (1986).

Subsequently, Childs (1989) adapted the bulk-flow model which was developed for the analysis of fluid-induced forces in seals to evaluate the rotordynamic forces due to these leakage flows. The magnitude and overall form of the model predictions are consistent with the experimental data. In particular, the model also predicts positive, rotordynamically destabilizing tangential forces over a range of positive whirl ratios. However, Childs' theory yielded some unusual results including peaks in the rotordynamic forces at particular positive whirl ratios. It is clear that a detailed comparison of model predictions with experimental measurement remains to be made and is one of the purposes of the present program.

3 Leakage Flow Test Apparatus

A detailed description of the test facility, can be found in many of the references (Chamieh, 1983; Adkins, 1986; Jery, 1986; Arndt, 1988; Franz, 1989), so only a brief description will be given here. The experiments were conducted in the Rotor Force Test Facility (RFTF), which was constructed to study fluid induced forces on an impeller whirling around the machine axis of rotation. The experimental objective was to impose well-controlled rotational and whirl motions on a very stiff impeller/shaft system and to measure directly the resulting force on the impeller. This is accomplished by an eccentric

Nomenclature

$[A^*]$ = rotordynamic matrix
$[A]$ = rotordynamic matrix normalized by $\rho\pi\omega^2 R_2^3 L$
C,c = rotordynamic damping coefficients normalized by $\rho\pi\omega R_2^3 L$
$F^*(t)$ = hydrodynamic forces
$F(t)$ = hydrodynamic forces normalized by $\rho\pi\omega^2 R_2^3 L\epsilon/R_2$
$F_x^*(t), F_y^*(t)$ = lateral forces on the rotating shroud in the stationary laboratory frame
$F_x(t), F_y(t)$ = lateral forces on the rotating shroud in the stationary laboratory frame normalized by $\rho\pi\omega^2 R_2^3 L\epsilon/R_2$
F_{ox}^*, F_{oy}^* = steady hydrodynamic forces
F_{ox}, F_{oy} = steady hydrodynamic forces normalized by $\rho\pi\omega^2 R_2^3 L$
$F_n^*(t), F_t^*(t)$ = unsteady hydrodynamic forces
$F_n(t), F_t(t)$ = unsteady hydrodynamic forces normalized by $\rho\pi\omega^2 R_2^3 L\epsilon/R_2$
H = shroud clearance between rotor and casing
K,k = rotordynamic stiffness coefficients normalized by $\rho\pi\omega^2 R_2^3 L$
L = axial length of the shroud
M,m = rotordynamic inertial coefficients normalized by $\rho\pi R_2^3 L$
Q = volume flow rate
R = shroud radius
Re_φ = axial flow Reynolds number, $2HU_s/\nu$
Re_ω = Reynolds number based on tip speed, $\omega R_2^2/\nu$
t = time
$x^*(t)$ = instantaneous displacement in the x direction normalized by the leakage inlet radius, R_2
$y^*(t)$ = instantaneous displacement in the y direction normalized by the leakage inlet radius, R_2
δ = offset or distance between the center of the whirl orbit and the center of the stationary casing
ϵ = eccentricity or radius of the whirl motion
ν = dynamic viscosity of the fluid
ρ = density of the fluid
ϕ = flow coefficient, $Q/2\pi R_2^2 H\omega$
ω = radian frequency of rotor rotation
Ω = radian frequency of whirl motion

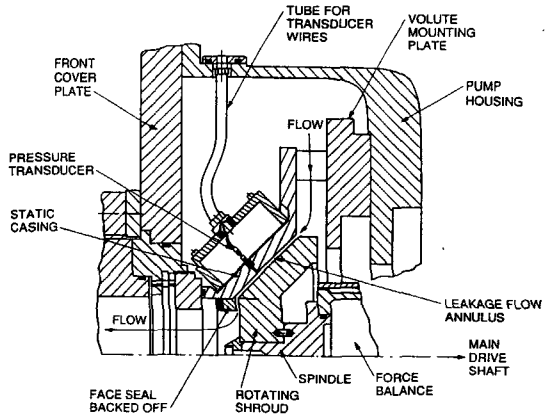

Fig. 2 Layout of the leakage flow test apparatus for installation in the Rotor Force Test Facility (Zhuang, 1989)

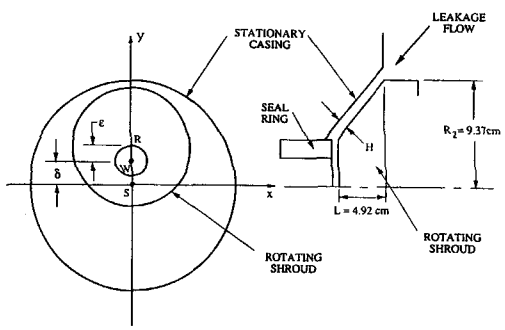

Fig. 3 Schematic of the whirling shroud where *S* is the center of the stationary casing, *R* is the center of the rotating shroud, *W* is the center of the whirl orbit along which *R* travels, $WR=\epsilon$ is the eccentricity and $WS=\delta$ is the offset

drive mechanism which superposes a circular orbit on the basic rotation. The shroud is mounted on a spindle attached to the rotating force balance (Jery et al., 1985; Franz et al., 1989), which measures the forces directly on the shroud. The experimental apparatus sketched in Fig. 2 was designed and constructed to simulate the leakage flow along the shroud from the impeller discharge to the impeller inlet (Zhuang, 1989; Guinzburg et al., 1990). The clearance between the rotating shroud and the stationary casing can be varied by both axial and radial adjustment of the stationary casing. For the present experiment, the initial geometric configuration consists of a straight annular gap inclined at an angle of 45 deg to the axis of rotation. The schematic in Fig. 3 shows the clearance in the centered position when the centers of the shroud and the casing both coincide. In order to model losses in the flow, an adjustable face seal was used (refer to Fig. 2). In the present experiment, the face seal clearance permits the pressure drop to be adjusted separately from the flowrate.

The flow through the leakage path is generated by an auxiliary pump and the selection of the flow rates through the leakage path was based on performance characteristics of a typical centrifugal pump. The shroud can be driven at speeds up to 3500 rpm and a circular whirl motion with a frequency up to 1800 rpm can be superimposed on the basic rotation. The eccentric drive mechanism permits testing with the amplitude of the whirl motion or eccentricity, ϵ adjustable from 0.000 cm to 0.152 cm. The distance from the center of the whirl orbit to the center of the casing, termed the fixed offset, δ is also variable. So concentric and nonconcentric circular whirl orbits could be investigated. However, the present experiments are confined to the case of zero offset. Further details of the experimental equipment can be found in Guinzburg (1992).

The results from these experiments will be presented nondimensionally by dividing the forces by $\rho\pi\omega^2R_2^3L\epsilon/R_2$. In most pumps L, the axial length of the leakage path and the impeller discharge width are comparable and hence, the dimensionless data from the leakage flow tests may be qualitatively compared with that from the impeller tests.

4 Experimental Results for Rotordynamic Forces

Typical experimental measurements of the dimensionless normal and tangential forces, F_n and F_t, will be presented in this section. The fluid medium in which the experiments were conducted was water. The rotordynamic results from the force balance measurements were obtained for different rotating speeds of 500, 1000, 2000 rpm, different leakage flow rates (zero to 50 gpm), three different clearances, H, and two eccentricities, ϵ. Another parameter which has an effect on the results is the swirl velocity at the inlet to the leakage flow. The present paper will be confined to a presentation of the results for zero inlet swirl, since the effect of swirl is dealt with in another paper (Guinzburg et al., 1992). The range of rotational Reynolds numbers was 462×10^3–1851×10^3 and the range of axial flow Reynolds numbers was 2136–8546. While the rotational Reynolds numbers for the experimental flows are clearly in the developed turbulent regime, it is possible that the axial flow Reynolds numbers were too small to manifest the kind of resonances predicted by Childs.

The components of the generalized hydrodynamic force matrix that result when the impeller whirls in an eccentric orbit of 0.0254 cm, at 1000 rpm, and a clearance of 0.140 cm are shown in Fig. 4. Note that the general form and magnitude of the data is very similar to that obtained for impellers by Jery (1986) and Adkins (1986) and to that from Childs' model in the absence of the "resonance." One of the most significant features of these results is the range of positive whirl frequency ratios within which the tangential force is positive and therefore potentially destabilizing rotordynamically. Note also that a positive normal force is directed outward and would tend to increase the displacement of the impeller. The parabolic shape of the normal force curve results from the added mass of the fluid.

Since the data of Figs. 4 and 5 were obtained under conditions which were the same except for the magnitude of the eccentricity, ϵ it is reassuring to note the similarity between the two sets of data. Evidently these experiments lie within the linear regime of small eccentricities (note that the assumption of linearity was implicit in Eq. (1)). Other experiments were performed for the same conditions as Figs. 4 and 5 except that the rotor speeds are 500 rpm and 2000 rpm with satisfactory agreement (Guinzburg, 1992). It is somewhat startling to find that the linear regime extends up to and beyond the point where the eccentricity is 60 percent of the clearance.

In Figs. 4 and 5, the effect of flow rate on the normal force is clearer than its effect on the tangential force. Clearly the Bernoulli effect on the normal force increases with increasing flow at both positive and negative whirl frequency ratios. It would also appear that the positive tangential forces at small positive whirl frequency ratios are smallest at the highest flow rate and therefore increasing the flow is marginally stabilizing. From experiments performed with different clearances, the forces are roughly inversely proportional to the clearance (Guinzburg, 1992). For the same eccentricity and two different clearances, the smaller clearance generates larger perturbations in the flow which accentuates the acceleration in the fluid and increases the pressure differences.

It is interesting to compare the magnitudes of the forces with previous results obtained for a real centrifugal impeller in the same facility. The data presented by Franz et al. (1989) for a Byron Jackson centrifugal pump were obtained with an eccentricity of 1.25 mm which is significantly larger than the present

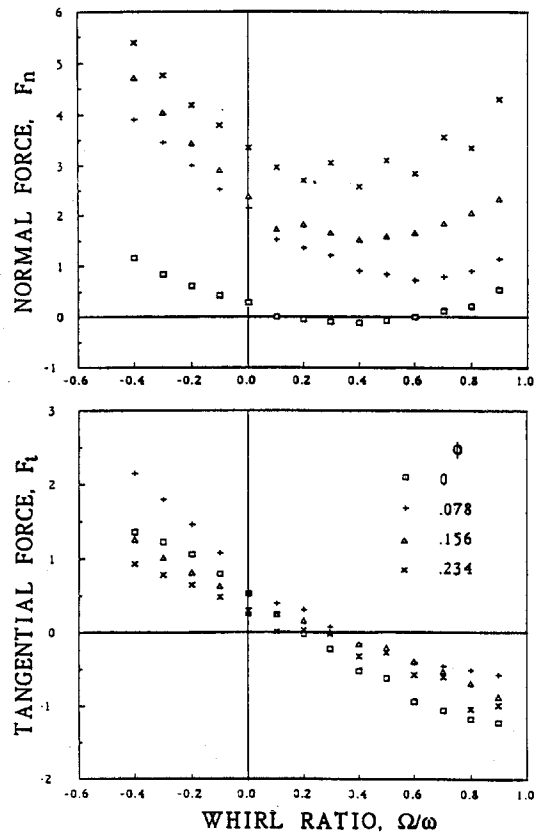

Fig. 4 Dimensionless normal and tangential forces normalized by $\rho\pi\omega^2 R_2^3 L\epsilon/R_2$ at 1000 rpm, for an eccentricity $\epsilon = 0.0254$ cm, a clearance $H = 0.140$ cm, offset $\delta = 0$ and different flow rates as follows: 0 l/s ($\phi = 0$), 0.631 l/s ($\phi = 0.078$), 1.262 l/s ($\phi = 0.156$), 1.892 l/s ($\phi = 0.234$). Uncertainty expressed as a standard deviation: F_n, $F_t \pm 0.05$.

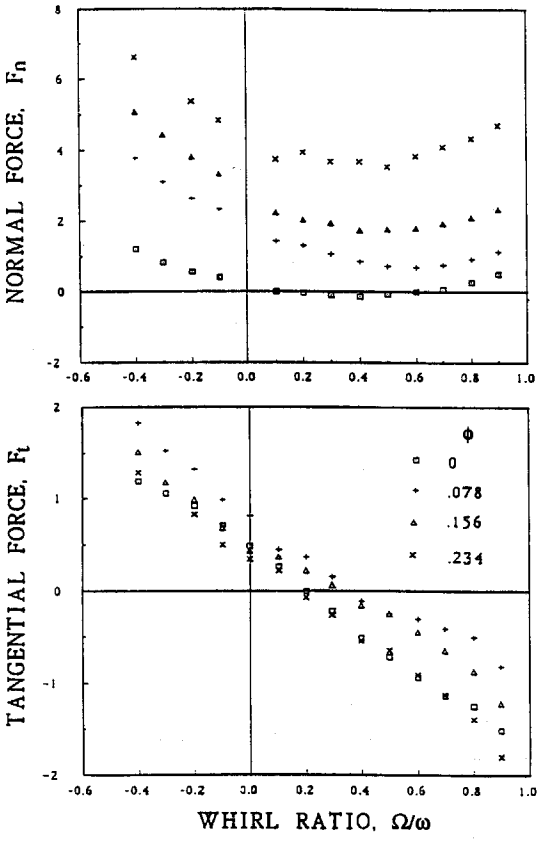

Fig. 5 Dimensionless normal and tangential forces normalized by $\rho\pi\omega^2 R_2^3 L\epsilon/R_2$ for zero inlet swirl at 1000 rpm, for an eccentricity $\epsilon = 0.0118$ cm, a clearance $H = 0.140$ cm, offset $\delta = 0$ and different flow rates as follows: 0 l/s ($\phi = 0$), 0.631 l/s ($\phi = 0.078$), 1.262 l/s ($\phi = 0.156$), 1.892 l/s ($\phi = 0.234$). Uncertainty expressed as a standard deviation: F_n, $F_t \pm 0.05$.

value of 0.254 mm. Thus, it is appropriate to compare the "stiffnesses" F_n^*/ϵ and F_t^*/ϵ rather than the forces themselves. At zero whirl frequency ratio the present data for a clearance of 1.40 mm (or 4.24 mm), yields values of 2.8 KN/m (or 0.46 KN/m) and 7.6 KN/m (or 1.88 KN/m) respectively compared to 6.8 KN/m and 2.28 KN/m for the data of Franz et al. (1989). Though the geometries of the leakage pathways are quite different this still suggests that the contribution of the shroud leakage flow to the rotordynamic forces is substantial.

The Reynolds number effect is investigated by examining the results of experiments which were identical except that the velocities (rotational, whirl and flowrate) were all increased or decreased by the same factor (Guinzburg, 1992). Hence, for example, the flow coefficients were identical. It was found that the coefficients do not change substantially as Reynolds number $\mathrm{Re}_\omega = \omega R_2^2/\nu$ increases. In the earlier work of Zhuang (1989), the normal and tangential forces were seen to decrease slightly as the Reynolds number increased. Those experiments were performed for no flow conditions. The present finding is consistent with the measurements of Jery (1987) on a centrifugal pump which were not affected by the Reynolds number.

5 Rotordynamic Coefficients

Conventionally, rotordynamics represent the force matrix by subdividing into components which depend on the orbit position (x,y), the orbit velocity $(\dot{x},\dot{y})$ and the orbit acceleration $(\ddot{x},\ddot{y})$. It is convenient for analytical purposes to evaluate these components by fitting quadratics to the experimental data. Though the functional dependence of F_n on the whirl frequency ratio is not necessarily quadratic and that of F_t is not necessarily linear, it is nevertheless of value to the rotordynamicists to fit the data of the figures from the previous section to the following expressions:

$$F_n = M\left(\frac{\Omega}{\omega}\right)^2 - c\left(\frac{\Omega}{\omega}\right) - K$$

$$F_t = +m\left(\frac{\Omega}{\omega}\right)^2 - C\left(\frac{\Omega}{\omega}\right) + k \qquad (8)$$

where M, C, c, K, k are the dimensionless direct added mass (M), direct damping (C), cross-coupled damping (c), direct stiffness (K) and cross-coupled stiffness (k). The cross-coupled added mass (m) is omitted for simplicity, since a linear fit for F_t is adequate. From a stability point of view, the tangential force is most interesting; a positive cross-coupled stiffness is destabilizing because it drives the forward orbital motion of the rotor. Positive direct damping and negative cross-coupled stiffness are stabilizing because they oppose orbital motion.

6 Discussion of Results

The dimensionless rotordynamic coefficients, which were obtained by curve fitting the present experimental data, are presented in graphical form in Fig. 6 for a wide range of conditions; the coefficients are plotted against the flow coefficient, ϕ. Various effects such as speed, eccentricity and shroud clearance are shown together in Fig. 6 in order that the global effect on each coefficient with increasing leakage flow can be seen. A large negative stiffness results in a positive normal force which would tend to increase the radius of the orbital motion; increasing the leakage flow increases this force. On the other hand, a positive cross-coupled stiffness would result in the flow being destabilizing because it drives the forward

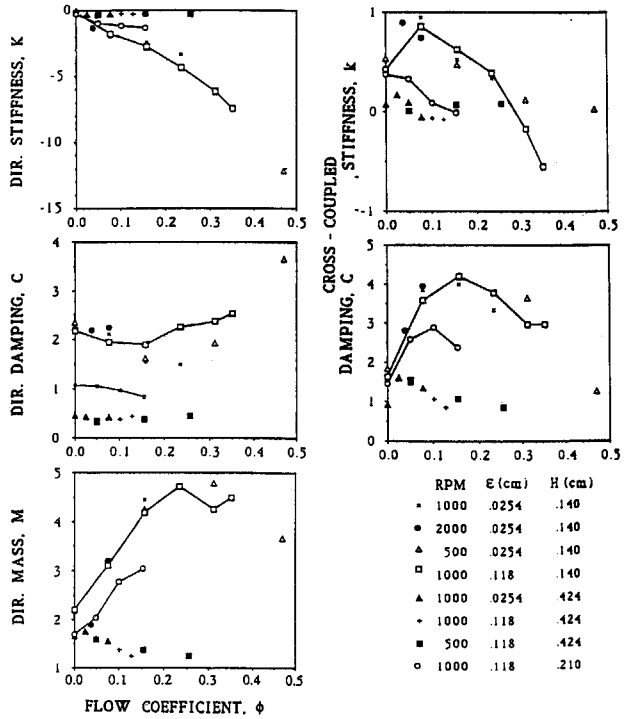

Fig. 6 Rotordynamic coefficients for different experimental conditions as a function of the flow coefficient

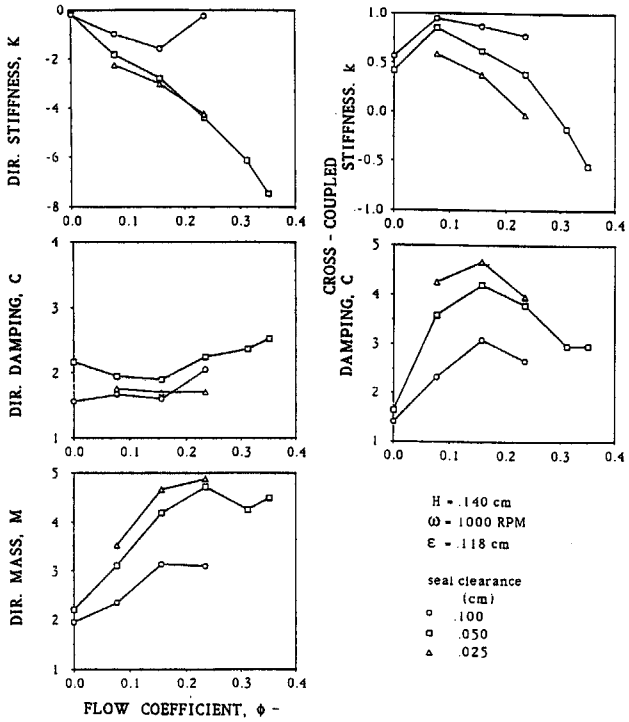

Fig. 7 Rotordynamic coefficients showing the effect of seal clearance as a function of flow coefficient for 1000 rpm and an eccentricity of 0.118 cm

orbital motion of the rotor so as to encourage whirl. The leakage flow is stabilizing in that the tangential force decreases with leakage flow. However, direct damping decreases slightly with flow, so the tangential force increases and the flow would therefore be less stabilizing. Below a flow coefficient of 0.7, direct damping is negative so the flow would encourage whirl. At higher flow rates, direct damping begins to increase and since this decreases the tangential force, the flow is stabilizing. However, these flow rates are much higher than realistic leakage flow rates in centrifugal pumps. The effect of the coefficients relating to the normal force is as follows. As the flow increases, the cross-coupled damping decreases slightly and the added mass term increases, thus contributing to a larger normal force. In other words, inertial motion would discourage orbital motion of the impeller but drive the impeller in the direction of displacement. It is interesting to note that at higher flow rates, the trend of the added mass changes.

In Fig. 6, the results for an eccentricity of 0.0254 cm and a clearance of 0.140 cm (obtained for a range of shaft speeds from 500 rpm to 2000 rpm) are seen to be independent of speed. Similar results were obtained with the same clearance but with a higher eccentricity of 0.118 cm (Guinzburg, 1992). This is simply another demonstration that the nondimensionalization of the forces with respect to speed is appropriate and that the Reynolds number effects are small.

The effect of eccentricity can be seen in Fig. 6 by examining the two sets of data (two different eccentricities) at 1000 rpm and a clearance of 0.140 cm. Even when the shroud clearance is of the same order of magnitude as the eccentricity, the results are still in the linear regime. Thus the magnitude of the eccentricity has no effect on the rotordynamic coefficients provided the latter are properly normalized.

The effect of the clearance between the rotating shroud and the stationary casing on the rotordynamic coefficients will next be presented for a speed of 1000 rpm and three clearances: 0.140, 0.212, and 0.424 cm. As the clearance is decreased, the stiffness and hence the normal force increases, which would drive the motion into a larger orbit. As the cross-coupled stiffness increases so does the tangential force and therefore the flow becomes more destabilizing. However, the direct damping acts in competition with k, because it increases as the clearance decreases. Rotordynamically speaking, the net effect is that a smaller force is generated with a larger clearance. The seal clearance also has an effect on the rotordynamic coefficients and this effect is presented in Fig. 7. In practice such a change could occur as a result of wear. Indeed the adjustable seal ring was used (Fig. 2) to model such effects. Measurements were obtained for face seal clearances of 0.0254 cm, 0.051 cm and 0.1016 cm. The larger seal clearance exhibits a smaller normal force and the tangential force is larger, which therefore decreases the range of destabilization. In other words, the range of positive whirl frequency ratios for which the tangential force is positive is decreased. The direct stiffness and the direct damping change so as to decrease the normal force which is in competition with the effect of the cross-coupled damping. The tangential force increases as a result of the cross-coupled stiffness, but the effect of the direct damping is not clear. So it would seem that wear in the seal is rotordynamically destabilizing.

7 Rotordynamic Stability

A convenient measure of rotordynamic stability is the ratio of cross-coupled stiffness to direct damping k/C, known as the whirl ratio. This provides an estimate of the whirl frequency ratio at which the force would no longer be destabilizing. Indeed, if the tangential force data lay exactly on a straight line, it would be exactly that whirl frequency ratio which corresponded to zero tangential force. Thus, reducing k/C improves the stability of the rotor system. As with the rotordynamic coefficients, the whirl ratios obtained from the present experiments are independent of rpm. Figure 8 also shows that as the clearance is decreased for a given flow rate, the whirl ratio increases. This is similar to the conclusion of Hawkins and Childs (1988) who showed that, in annular seals, decreasing the clearance increases the stability. The effect of increasing the seal clearance, illustrated in Fig. 9, is to decrease the whirl ratio.

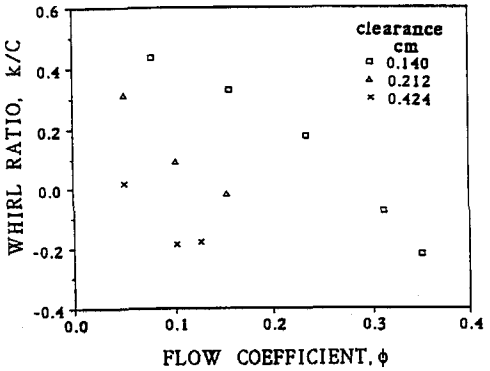

Fig. 8 Whirl ratio for an eccentricity $\epsilon = 0.118$ cm, speed of 1000 rpm, offset $\delta = 0$ and various clearances as a function of flow coefficient

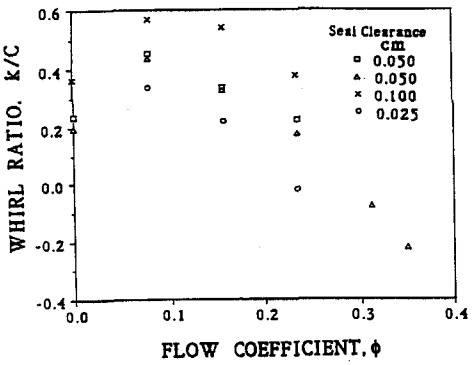

Fig. 9 Whirl ratio for an eccentricity $\epsilon = 0.118$ cm, speed of 1000 rpm, clearance $H = 0.140$ cm, offset $\delta = 0$ and various seal clearances as a function of flow coefficient

The whirl ratio from the results of Bolleter et al. (1989) gives surprisingly different results from the present research. For the total impeller, the whirl ratio is 1.4; for the seal the whirl ratio is 0.85 and for the difference of these contributions, the ratio is 2.26. The range for the results of the present experiments is smaller (-0.12 to 0.45). The discrepancies can be traced to differences in the cross-coupled stiffness and the direct damping, both of which are substantially larger in Bolleter et al. (1989) than in the present experiments.

8 Conclusions

A review of the existing experimental and analytical results shows that the discharge-to-suction leakage flow in a centrifugal pump can contribute substantially to the fluid-induced rotordynamic forces for that turbomachine. This motivated the current experimental study of leakage flows between the shroud and the stationary casing of a centrifugal pump and their rotordynamic effects. Experimental results for simulated leakage flows of rather simple geometry are presented for different whirl frequencies, eccentricities, clearances and flow rates. As with previous results for impellers, the forces scaled with the square of the rotor speed. The functional dependence on whirl frequency to rotating frequency ratio (termed the whirl frequency ratio) is very similar to that measured in experiments and to that predicted in the theoretical work of Childs.

Two sets of results taken at different eccentricities yield quite similar nondimensional rotordynamic forces indicating that the experiments lie within a linear regime. The dimensionless forces are found to be functions not only of the whirl frequency ratio but also of the flow rate and of the clearance. A region of forward whirl for which the average tangential force is destabilizing, was found. This region decreased with the flow coefficient for the leakage flow. While the dependence on the shroud clearance is not simple, it would appear that the dimensionless rotordynamic forces are roughly inversely proportional to the clearance. The change with the discharge resistance was somewhat more complicated. Finally, the tests showed none of the "resonances" predicted by the bulk-flow model proposed by Childs (1989).

Acknowledgments

The assistance provided by F. Zhuang, A. Bhattacharyya, F. Rahman, and Sandor Nagy with the experimental program is greatly appreciated. We would also like to thank NASA George Marshall Space Flight Center for support under NASA grant NAG8-118.

References

Adkins, D. E., 1986, "Analyses of Hydrodynamic Forces on Centrifugal Pump Impellers," Ph.D. thesis, California Institute of Technology, Pasadena, CA.

Adkins, D. R., and Brennen, C. E., 1988, "Analyses of Hydrodynamic Radial Forces on Centrifugal Pump Impellers," ASME JOURNAL OF FLUIDS ENGINEERING, Vol. 110, No. 1, pp. 20–28.

Bolleter, U., Wyss, A., Welte, I., and Stürchler, R., 1987, "Measurement of Hydrodynamic Interaction Matrices of Boiler Feed Pump Impellers," ASME *Journal of Vibration, Acoustics, Stress, and Reliability in Design*, Vol. 109, pp. 144–151.

Bolleter, U., Leibundgut, E., and Stürchler, R., 1989, "Hydraulic Interaction and Excitation Forces of High Head Pump Impeller," *Pumping Machinery*, Vol. 81, 3rd Joint ASCE/ASME Mechanics Conference, UCSD, July 9–12, pp. 187–193.

Chamieh, D. S., 1983, "Forces on a Whirling Centrifugal Pump-Impeller," Ph.D. thesis, Division of Engineering and Applied Science, California Institute of Technology, Pasadena, CA.

Chamieh, D. S., Acosta, A. J., Brennen, C. E., and Caughey, T. K., 1985, "Experimental Measurements of Hydrodynamic Radial Forces and Stiffness Matrices for a Centrifugal Pump-Impeller," ASME JOURNAL OF FLUIDS ENGINEERING, Vol. 107, No. 3, pp. 307–315.

Childs, D. W., 1989, "Fluid Structure Interaction Forces at Pump-Impeller-Shroud Surfaces for Rotordynamic Calculations," ASME *Journal of Vibration, Acoustics, Stress, and Reliability in Design*, Vol. 111, pp. 216–225.

Domm, U., and Hergt, P., 1970, "Radial Forces on Impeller of Volute Casing Pumps," *Flow Research on Blading*, L. S. Dzung, ed., Elsevier Publ. Co., Netherlands, pp. 305–321.

Franz, R., Acosta, A. J., Brennen, C. E., and Caughey, T. K., 1989, "The Rotordynamic Forces on a Centrifugal Pump Impeller in the Presence of Cavitation," *Proceedings of 3rd Joint ASCE/ASME Mechanics Conference*, UCSD, July, *Pumping Machinery*, Vol. 81, pp. 205–212.

Guinzburg, A., Brennen, C. E., Acosta, A. J., and Caughey, T. K., 1990, "Rotordynamic Forces Generated By Discharge-to-Suction Leakage Flows in Centrifugal Pumps," NASA CP-3092.

Guinzburg, A., Brennen, C. E., Acosta, A. J., and Caughey, T. K., 1990, "Measurements of the Rotordynamic Shroud Forces for Centrifugal Pumps," ASME Turbomachinery Forum, Toronto, Canada, June.

Guinzburg, A., 1992, "Rotordynamic Forces Generated By Discharge-to-Suction Leakage Flows in Centrifugal Pumps," Ph.D. thesis, Division of Engineering and Applied Science, California Institute of Technology, Pasadena, CA.

Guinzburg, A., Brennen, C. E., Acosta, A. J., and Caughey, T. K., 1992, "The Effect of Inlet Swirl on the Rotordynamic Shroud Forces in a Centrifugal Pump," Presented at the ASME Turbo Expo, June.

Hawkins, L., and Childs, D. W., 1988, "Experimental Results for Labyrinth Gas Seals With Honeycomb Stators: Comparisons to Smooth-Stator Seals and Theoretical Predictions," 3rd Conference on Advanced Earth-to-Orbit Propulsion Technology, Huntsville, Alabama, May, pp. 94–111.

Hergt, P., and Krieger, P., 1969–70, "Radial Forces in Centrifugal Pumps With Guide Vanes," *Proceedings Institute of Mechanical Engineers*, Vol. 184, Part 3N, pp. 101–107.

Jery, B., 1986, "Experimental Study of Unsteady Hydrodynamic Force Matrices on Whirling Centrifugal Pump Impellers," Ph.D. thesis, California Institute of Technology.

Jery, B., Acosta, A. J., Brennen, C. E., and Caughey, T. K., 1985, "Forces on Centrifugal Pump Impellers," *Second International Pump Symposium*, Houston, TX, April 29–May 2.

Zhuang, F., 1989, "Experimental Investigation of the Hydrodynamic Forces on the Shroud of a Centrifugal Pump Impeller," E249.9, Division of Engineering and Applied Science, California Institute of Technology.